INSAR OBSERVATIONS OF CRUSTAL DEFORMATION MECHANICS IN THE INTERIOR OF THE PUNA PLATEAU OF THE SOUTHERN CENTRAL ANDES

Felix Eckelmann [(1)], Mahdi Motagh [(1)], Bodo Bookhagen [(2)], Manfred Strecker[(3)]

[(1)] Department of Remote Sensing, Helmholtz Centre Potsdam, German Research Centre for Geosciences, D-14473 Potsdam, Germany. Email: *feckel@gfz-potsdam.de; mahdi.motagh@gfz-potsdam.de.*
[(2)] Geography Department, University of California, Santa Barbara, CA 93106-460, United States. Email: bodo@eri.ucsb.edu.
[(3)] Institute of Earth and Environmental Science, University of Potsdam, D-14476 Potsdam. Email: strecker@geo.uni-potsdam.de.

ABSTRACT

Crustal deformation evidences in the orogenic interior of the Southern Central Andes at different time scales are observed by applying ENVISAT InSAR time series from 2005 - 2009 and differential GPS data taken in the study area of the palaeo-lake Salar de Pocitos (24.5°S, 67°W, 3650 m asl). Ongoing shortening in the region from the Tertiary to the present-day is indicated by an uplift of Quaternary palaeo-lake terraces of about 4 to 5m within the last 44ka as well as by the growth of an anticline in Tertiary sediments and the reactivation of the reverse-fault bounded Sierra de Macón, both with uplift rates of 2 - 5mm/a. In summary, this study emphasizes the diachronous and spatially disparate character of the tectonic regime at the Puna Plateau.

1. INTRODUCTION

The Cenozoic Andes are the dominating geologic structure of the South American continent fundamentally influencing atmospheric circulation of the southern hemisphere [1]. Being characterized by a N-S elongation of approx. 7000km and peak elevations in excess of 6km, the Andes constitute one of the largest and even youngest orogens on Earth. Non-collisional convergence with current rates of about 10cm/a at the active western margin of the South American continent is associated with the eastward subduction of the oceanic Nazca Plate [2]. The fact that the Andes were uplifted in the absence of continental collision in addition to the coeval occurrence of shortening and extension processes makes them an ideal site for studying tectonic histories at different temporal and spatial scales. While long-term deformation characteristics in mountain belts such as unconformities or vertical stacking are often well expressed by structures preserved in the bedrock, it is difficult to characterize very young deformation phenomena. However, a primary tool in detecting relatively recent deformation resolved at mm-scale-accuracy is provided by **S**nythetic **A**perture **R**adar (SAR)-systems [3]. The technique of SAR interferometry has become widely accepted in geologic applications for more than a decade, e.g. [4]; [5]; [6]; [7]. These InSAR methods afford studying temporal evolution of displacement signals in short repetition cycles and thus highly contribute to the understanding of deformation dynamics, e.g. [8]. This study aims to characterize the degree of current crustal deformation in the interior of the Southern Central Andes, at the Puna Plateau in NW Argentina. Contrary to previous geologic investigations that suggested widespread, neotectonic extension on the plateau, e.g. [9], [10], the combined analysis of InSAR observations with differential Global Positioning System (dGPS) measurements of deformed lake terraces at the Salar de Pocitos in this study will demonstrate the protracted compressional tectonic regime at the Puna Plateau since the Tertiary.

2. GEOLOGIC SETTING

The Southern Central Andes extend to a latitude range from 22° to 27° S including Bolivia, Chile and NW Argentina. This part of the Andes is subdivided into several morphotectonic provinces (**Fig. 1**) striking parallel to the meridional trend of the orogen and thus

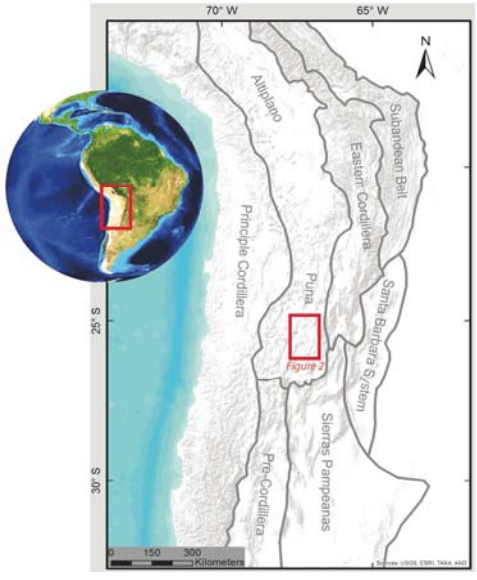

Figure 1. Morphotectonic provinces of the Southern Central Andes; after [12].

Proc. 'ESA Living Planet Symposium 2013', Edinburgh, UK 9–13 September 2013 (ESA SP-722, December 2013)

perpendicular to regional moisture-bearing winds, which emphasizes the strong climatic impact of the Andes in South America [11]. The target area in this study is the hyperarid, central Puna Plateau with an average elevation of 3.7km in the interior of the Southern Central Andes. Together with its northern continuation, the Bolivian Altiplano, it forms the second largest orogenic plateau on Earth [13]. But in contrast to the broad, flat Altiplano [14], the Puna Plateau is mainly characterized by an arrangement of internally drained, intervening basins and high-angle, reverse-fault bounded ranges, constituting a compressional basin-and-range morphology [15]. Moreover, the Puna exhibits a very low level of seismicity [16]. Subduction of oceanic crust has been dominating the tectonic regime of western South America since the Cretaceous, e.g. [2], [17] whereas first uplift signals has been noted for Eo-Oligocene time [18], [19]. Two distinct kinematic regimes have dominated Late Cenozoic deformation on the Puna Plateau. The older regime associated with NW-SE horizontal contraction that was active from at least 13 to 9Ma [17] and possibly even longer [20] is regarded as being responsible for the major topographic uplift of the Plateau [21]. This regime of vertical extension and horizontal contraction was displaced by a dominantly horizontal NNW-SSE directed extension and horizontal NE-SW contraction in the Late Miocene which is regarded as being active at present-day [9], [10]. The

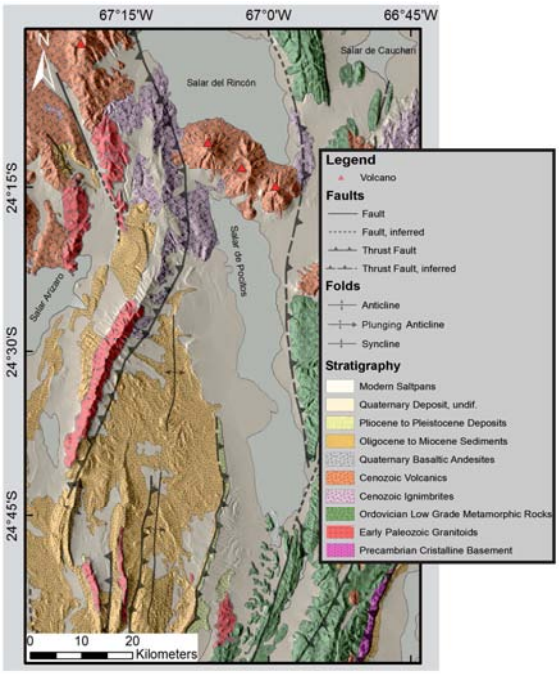

Figure 2. Geologic map of the study area: Salar de Pocitos; after [12].

temporal and spatial evolution of this changeover is not well understood and has been linked to a combination of different processes as e.g. lithospheric delamination, a reorganization of plate-tectonic boundary conditions or gravitation-driven extensional spreading, e.g. [2], [20], [22], [23]. In these models, neotectonic shortening is regarded as only continuing along the plateau margins and in the foreland, e.g. [9]. The area of investigation in this study is the Salar de Pocitos Basin being located at 24.5° S latitude and 67° W longitude. This hydrologically-closed basin constitutes a N-S oriented salt-flat depression with a minimum elevation of 3650m asl. Large geologic structures such as an anticline involving E-tilted Tertiary and Quaternary sediments as well as the Sierra de Macón thrust fault are bordering this basin to the west [24], whereas it is limited by a reverse-faulted range to the east (**Fig. 2).** Quaternary lacustrine shorelines run parallel along the margins of the basin, suggesting oscillations of palaeo-lakes [25].

3. METHODS

3.1. DGPS Measurements

The Salar de Pocitos constitutes the vestige of a palaeo-lake and hence exhibits many geomorphologic markers including lacustrine terraces. These terraces record changing lake levels on the one hand but also subsequent deformation processes that have impacted this region on the other hand. Since the reconstruction of different evolutionary stages of the palaeo-lake and the analysis of tectonic tilting of the terraces requires high-precision in the vertical dimension, investigations on geomorphologic features at the Salar de Pocitos were carried out by means of differential GPS measurements. This technique extends the classical GPS approach by using a stationary base (reference) station coupled with one or various mobile rover receivers which affords an accuracy at a resolution of tenth`s of millimetres [26].

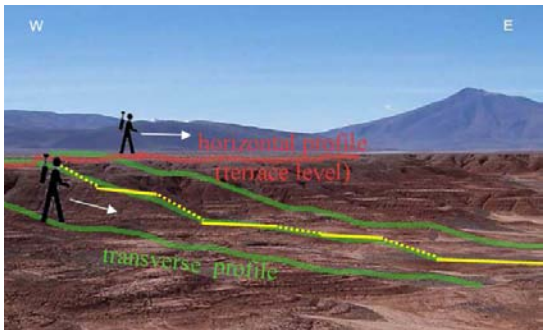

Figure 3. Differential GPS field measurements with the yellow line schematically displaying the staircase-like morphology of different terrace generations.

For that purpose, one Trimble Pathfinder ProXRS GPS device was installed onto a tripod to serve as fixed base-station continuously logging data over a time period of seven weeks, whereas another ProXRS as well as one

ProXRT2 device were used as mobile rovers in the field. Hence, the position of the base station was precisely determined and satellite signal errors could be estimated and applied to the rovers by using a kinematic post-processing correction algorithm [27]. Differential GPS data were acquired by measuring parallel to the lacustrine terraces (horizontal profiles) as well as perpendicular to them (transverse profiles), which should reveal different palaeo-lake-highstands in a staircase-like morphology associated with variable slope geometry (**Fig 3**). Thus, more than 146,000 data points from over 180 different terraces were measured correctly and referenced to the WGS-84 ellipsoid.

3.2. InSAR Observations

For the purpose of observing ground deformation at the Pocitos Basin within the last decade, the method of SAR interferometry was applied. Fifteen SAR acquisitions from the ENVISAT satellite in a time period from 2005 to 2009 in a descending orbit mode were processed by using StaMPS software [28]. The basic concept of repeat-pass interferometry is the combination of two SAR-images acquired from identical orbits, but at distinct time. A change in phase of the transmitted pulse of these two SAR-images is an expression of ground displacement with a precision at millimeter scale [29]. This method requires the correction of influences of the viewing geometry to the interferometric phase, which was done by using precise orbit data provided by the ESA. Additionally, topographic correction was applied by using the 90-m-resolution SRTM-(Shuttle Radar Topography Mission) digital elevation model. Phase unwrapping was computed by the Snaphu unwrapper [30]. Moreover, a time-series approach was initiated in order to generate a combined deformation plot summarizing the results of all SAR-acquisitions within a certain subset. For areas exhibiting high correlation over time like the non-vegetated, hyperarid Pocitos Basin, typically the **S**mall **BA**seline **S**ubset (SBAS) method that aims to minimize perpendicular, temporal and Doppler baseline from a subset of images is applied [31]. Thus, independent SAR datasets were effectively combined based on a minimum-norm criterion for the baseline distribution and a network of a total of fifty interferograms could be generated [8]. This afforded the calculation of a deformation time-series for each coherent pixel and thus the estimation of an average ground displacement map (**Fig. 5**). A more detailed discussion of the SBAS approach is given in [32].

4. RESULTS

4.1. Field Results

In general, possible palaeo-lake-level highstands in arid basins are associated with prominent geomorphic structures such as gently sloping pediments cut by escarpment edges or a staircase-shaped topography at the margins of a palaeo-lake basin [33]. These geomorphic features can be observed in the study area, although their degree of preservation strongly varies throughout the basin. An independent elevation analysis based on dGPS measurements was carried out to verify these structures. In order to extract geomorphically and structurally meaningful conclusions from the dGPS data, measurements were separated into four main groups (north, south, west and east) according to terrace morphology and their spatial distribution. Height data in each of the four groups point to distinct elevation clusters characterized by a maximum of the probability density function, which are interpreted as representing terrace levels (**Fig. 4**). Thus, dGPS data reveal de facto at least three generations of terraces within a height range of 3653m (salar basel level) and the highest terrace level at about 3680m. Despite of showing

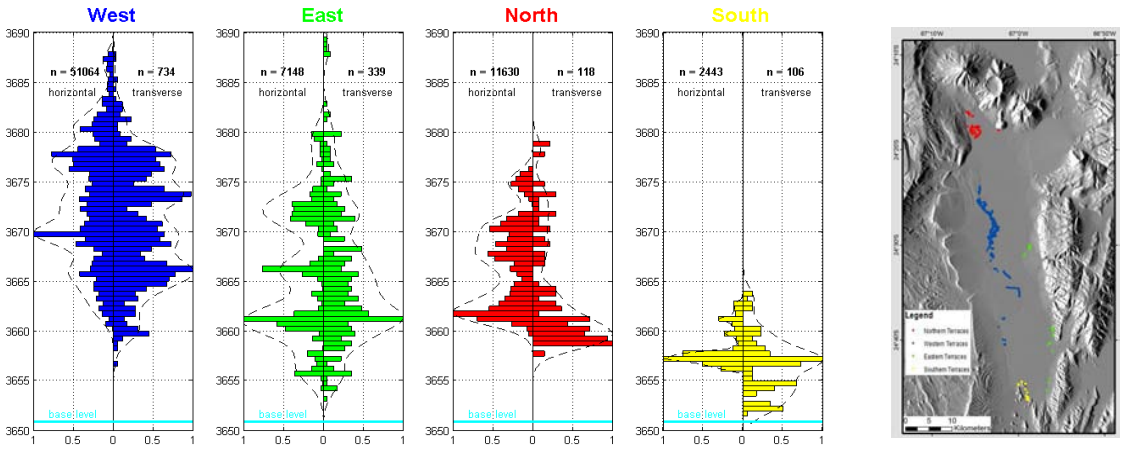

Figure 4. Left: Terrace height is plotted versus the normalized frequency of elevation overlain by a Kernel-smoothing probability density function (dashed line). Right: Location of measured terraces from each group - the median values for longitude and latitude were calculated.

different absolute elevations of terrace levels, the relative cluster-heights within the different groups are consistent, which affords the correlation of similar generations of palaeo-lake level highstands. But the northern and especially western part of the basin shows higher elevations in extent of 4-5m with respect to the east and south-eastern parts of the salar. Radiocarbon dating on a calcrete sample topping the uppermost terrace in the western part of the salar reveals an age of 40,180 (+1420/-1200) ^{14}C-a, which indicates that one of the palaeo-lake highstands must have reached a maximum extent at about 44ka ago. This age corresponds well to the Minchin wet phase that is observable in other salars in the region as well (Salar de Uyuni: e.g. [34]; Salar de Atacama: [25] and Lake Titicaca: e.g. [35]). In summary, principal elevation analysis indicates individual terrace levels at ~12m, ~17m and ~24m above the current base level of the salar at which the western and northern part of the salar is elevated in extent to 4 to 5m in respect to these levels.

4.2. InSAR Results

The recent deformation characteristics of the Salar de Pocitos region can be assessed based on processed InSAR data. A combined deformation map showing the average ground displacement rate per year calculated from all ENVISAT interferograms within the SBAS network in a time period from 2005 to 2009 is illustrated in **Fig. 5**. The velocity vector of each single pixel in this plot points towards the line of sight (LOS) of the satellite and cannot be splitted into vertical and horizontal components. As a general trend in the target area, uplift is prominent in the northwestern sector, whereas large-scale subsidence dominates the southeastern sector, both with rates of about 10mm/a. An important observation comes from the Tertiary sediments exposed in the area of the large anticline to the west of the salar as well as from the reverse fault-bounded Sierra de Macón (compare **Fig. 2**), which both exhibit a clear uplift signal in extent of up to 5mm/a as visible in the profiles in **Fig. 5**. The Quaternary alluvial fans at the eastern margin of the basin are characterized by slight subsidence which may reflect erosion processes. The signal arising at the salar surface is characterized by very high and also alternating rates and can thus be separated from the marginal areas of the Pocitos Basin and the ranges, which exhibit deformation rates of one order of magnitude lower. For that reason, a tectonically-driven source of ground displacement at the salar surface is very unlikely. The three volcanoes to the north of the Salar show subsidence signals which may arise from deflation processes due to inactivity.

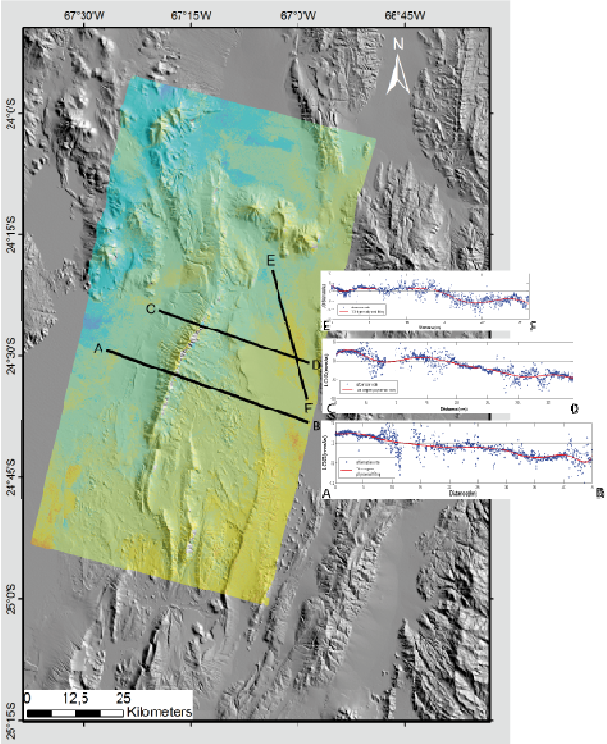

Figure 5. SBAS plot displaying the mean velocities of every single pixel (ENVISAT). The profiles plot the rate of deformation in mm/a versus the distance.

5. DISCUSSION

The combined analysis of dGPS measurements and InSAR satellite data provides the basis for a synoptic interpretation of the neotectonic deformation character of the Salar de Pocitos area. Overall, the area is characterized by present-day shortening, which contrasts with the widely held view that the Puna Plateau as a whole is currently subjected to extensional processes, while the plateau margins continue to be shortened [9], [10]. Evidences for a compressional tectonic regime exist at least since the Tertiary, in which large geologic structures to the west of the Salar de Pocitos as e.g. the reverse-fault bounded Sierra de Macón [24] were generated. These structures coincide well with the proposed models of predominant NNE-SSW thrust faulting during the Miocene and Pliocene, e.g. [17] [21] as also observable in other areas of the Puna, e.g. [18], [36], [37], [38]. A continued shortening for the Quaternary is indicated by the eastward tilt of the strata to the west of the salar as well as by the deformation patterns of Quaternary palaeo-lake terraces. Uplift of the terraces point to ongoing shortening at the Salar de Pocitos area even during the Late Pleistocene and Holocene. Differential GPS measurements and a dated calcrete sample from the uppermost terrace reveal that a tectonic shift in extent of 4 to 5m of the western margin of the salar must haven taken place since the last 44ka. The most recent manifestation of deformation and evidence for continued shortening in the region can be inferred from InSAR results. A large scale trend of uplift in the NW and subsidence in the SE of the target area may reflect active deformation and thus long-wavelength E-W directed shortening. Local

displacement velocities are may be associated with large geologic structures to the west of the Salar de Pocitos with uplift rates of 2 to 5mm/a in the area of the large anticline at 67°10' W longitude and at the reverse-fault bounded Sierra de Macón. Thus, these velocities may reflect an active growth of the anticline and associated fault activity at the Sierra de Macón. However, the rates seem to be quite high compared to the geologic rates derived from the dGPS results and thus may only reflect locally increased tectonic activity. Problems arising from atmospheric influences to the interferometric phase also have to be taken into account. But in general, ENVISAT time-series analysis indicate ongoing shortening in the interior of the plateau during the last decade. For that reason, InSAR results strongly support the hypothesis that not all sectors of the high plateau are undergoing extension at present day, which calls for a re-assessment of models assuming a plateau-wide shift from shortening to extension at the Puna [9], [10]. Moreover, this study additionally reveals important observations of the displacement behaviour at the salar interior. Thus, the highly alternating velocity rates of the salt flat may are associated with hydrologically and climatically driven volumetric changes of halite, which coincides well with already known relationships between vertical movements in salt flats and water availability in other areas of the Puna [39]. Those signals can clearly be separated from tectonic motion.

6. CONCLUSION

Taken together, this study demonstrates protracted shortening at the Puna Plateau since the Tertiary, based on the synoptic analysis of spaceborne SAR data and geomorphic field measurements with dGPS. The target area, the Salar de Pocitos, has been tectonically active over the last Millions of years, as indicated by large thrust structures from the Tertiary (Sierra de Macón), deformed Qaternary palaeo-lake terraces and very recent ground displacement rates. These evidences of deformation point towards a compressional tectonic regime at the Puna: dGPS measurements indicate an uplift in extent to 4 to 5m of palaeo-lake terraces within the last 44ka and InSAR analysis reveal uplift of large geologic structures to the west of the Salar de Pocitos and thus a growth of an anticline with rates of 2 - 5 mm/a as well as associated fault activity at the Sierra de Macón. These results emphasize the diachronous and spatially disparate character of the tectonic regime in the interior of the Southern Central Andes.

7. REFERENCES

1. Garreaud, R. D. (2009). The Andes climate and weather. Advances In Geosciences, **22**, 3-11.

2. Pardo-Casas, F. & P. Molnar (1987). Relative motion of the Nazca (Farallón) and South American Plates since Late Cretaceous time. Tectonics, **6**(3), 233-248.

3. Rosen, P.A., S. Hensley, I.R. Joughin, S.N. Madsen, E. Rodríguez & R.M. Goldstein (2000). Synthetic Aperture Radar Interferometry. Proceedings of the IEEE, **88**(3), 333-382.

4. Gabriel, A.K., R.M. Goldstein & H.A. Zebker (1989). Mapping small elevation changes over large areas: Differential radar interferometry. Journal of Geophysical Research: Solid Earth, **94**(B7), 9183–9191.

5. Massonnet, D. & K.L. Feigl (1998). Radar Interferometry and its application to changes in the earth`s surface. Reviews of Geophysics, **36**(4), 441-500.

6. Feigl, K.L., J. Gasperi, F. Sigmundsson & A. Rigo (2000). Crustal deformation near Hengill volcano, Iceland 1993–1998: Coupling between magmatic activity and faulting inferred from elastic modeling of satellite radar interferograms. Journal of Geophysical Research: Solid Earth, **105**(B11), 25655–25670.

7. Peltzer, G., F. Crampé, S. Hensley & P. Rosen (2001). Transient strain accumulation and fault interaction in the Eastern California shear zone. Geology, **29**(11), 975-978.

8. Lanari, R., O. Mora, M. Manunta, J.J. Mallorquí, P. Berardino & Eugenio Sansosti (2004). A Small-Baseline Approach for Investigating Deformations on Full-Resolution Differential SAR Interferograms. IEEE Transactions on Geoscience and Remote Sensing, **42**(7), 1377-1386.

9. Montero Lopez, M.C., F.D. Hongn, M.R. Strecker, R. Marrett, R. Seggiaro & M. Sudo (2010). Late Miocene–early Pliocene onset of N-S extension along the southern margin of theCentral Andean Puna Plateau: Evidence from magmatic, geochronological and structural observations. Tectonophysics, **494**, 48-63.

10. Schoenbohm, L. M. & M. R. Strecker (2009). Normal faulting along the southern margin of the Puna Plateau, northwest Argentina. Tectonics, **28**(5), TC5008, 1- 21.

11. Strecker, M.R., R.N. Alonso, B. Bookhagen, B. Carrapa, G.E. Hilley, E.R. Sobel & M.H. Trauth (2007). Tectonics and Climate of the Southern Central Andes. Annual Review of Earth Planetary Science, **35**, 747 -787.

12. Allmendinger, R.W., V.A. Ramos, T.E. Jordan, M. Palma & B.L. Isacks (1983). Paleogeography and Andean structural geometry, Northwest Argentina. Tectonics, **2**(1), 1-16.

13. Marrett, R.A., R.W. Allmendinger, R.N. Alonso & R.E. Drake (1994). Late Cenozoic tectonic evolution of the Puna Plateau and adjacent foreland, northwestern Argentine Andes. Journal of South American Earth Science, **7**(2), 179 – 207.

14. Whitman, D., B.L. Isacks & S. Mahlburg Kay (1996). Lithospheric structure and along-strike segmentation of the Central Andean Plateau: seismic Q, magmatism, flexure, topography and tectonics. Tectonophysics, **259**, 29-40.

15. Allmendinger, R.W., T.E. Jordan, S.M. Kay & B.L. Isacks (1997). The Evolution of the Altiplano-Puna Plateau of the Central Andes. Annual Review of Earth Planetary Science, **25**, 139-174.

16. Cahill, T. & B.L. Isaacks (1992). *Seismicity and Shape of the Subducted Nazca Plate.* Journal of Geophysical Research, **97**(B12), 503-529.

17. Cladouhos, T.T., R.W. Allmendinger, B. Coira & E. Farrar (1994). Late Cenozoic deformation in the Central Andes: fault kinematics from the northern Puna, northwestern Argentina and southwestern Bolivia. Journal of South American Earth Sciences, **7**(2), 209-228.

18. Carrapa, B., D. Adelmann, G.E. Hilley, E. Mortimer, E.R. Sobel & M.R. Strecker (2005). Oligocene range uplift and development of plateu morphology in the southern central Andes. Tectonics, **24**(4), TC40011, 1-19.

19. Hongn, F., C. del Papa, J. Powell, I. Petrinovic, R. Mon & V. Deraco (2007). Middle Eocene deformation and sedimentation in the Puna-Eastern Cordillera transition (23°-26°S): Control by preexisting heterogeneities on the pattern of initial Andean shortening. Geology, **35**(3), 271-274.

20. Marrett, R. & M.R. Strecker (2000). Response of intracontinental deformation in the central Andes to late Cenozoic reorganization of South American Plate motions. Tectonics, **19**(3), 452-467.

21. Allmendinger, R.W., M.R. Strecker, J.E. Eremchuk & P. Francis (1989). Neotectonic deformation of the southern Puna Plateau, northwestern Argentina. Journal of South American Earth Sciences, **2**(2), 111 – 130.

22. Allmendinger, R.W. (1986). Tectonic development, southeastern border of the Puna Plateau, northwestern Argentine Andes. Geological Society of American Bulletin, **97**(9), 1070-1082.

23. Kay, S.M., B. Coira a& J. Viramonte (1994). Young mafic back arc volcanic rocks as indicators of continental lithospheric delamination beneath the Argentine Puna plateau, central Andes. Journal of Geophysical Research, **99**(B12), 323-339.

24. Poma, S., S. Quenardelle, V. Litvak, E.B. Maisonnave & M. Koukharsky (2004). The Sierra de Macon, Plutonic expression of the Ordovician magmatic arc, Salta Province Argentina. Journal of South American Earth Sciences, **16**, 587–597.

25. Bobst, A.L., T.K. Lowenstein, T.E. Jordan, L.V. Godfrey, T.-L. Ku & S. Luo (2001). A 106 ka paleoclimate record from drill core of the Salarde Atacama, northern Chile. Palaeogeography, Palaeoclimatology, Palaeoecology, **173**, 21-42.

26. Mansfeld, W. (2010). Satellitenortung und Navigation: Grundlagen, Wirkungsweise und Anwendung globaler Satellitennavigationssysteme (3rd ed.). Vieweg+Teubner Verlag, Wiesbaden, pp. 203 - 210.

27. Koenig, F. & D. Wong (2007). Differential Global Positioning System (DGPS) Operation and Post-Processing Method for the Synchronous Impulse Reconstruction (SIRE) Radar. U.S. Army Research Laboratory, Adelphi, MD 20783-1197, Final Report ARL-TN-0281.

28. Hooper, A., K. Spaans, D. Bekaert, M.C. Cuenca, M. Arıkan & A. Oyen (2010). StaMPS/MTI Manual (Version 3.2). Delft University of Technology, Delft Institute of Earth Observation and Space Systems, The Netherlands.

29. Bürgmann, R., P.A. Rosen & E.J. Fielding (2000). Synthetic Aperture Radar Interferometry to measure Earth`s surface topography and its deformation. Annual Review of Earth Planetary Science, 28, 169-209.

30. Chen, C.W. & H.A. Zebker (2001). Network approaches to two-dimensional phase unwrapping: Intractability and two new algorithms. Journal of Optical Society of America, A17, 401−414.

31. Hooper, A. (2008). A multi-temporal InSAR method incorporating both persistent scatterer and small baseline approaches. Geophysical Research Letters, **35**(L16302), 1-5.

32. Berardino, P., G. Fornaro, R. Lanari & E. Sansosti (2002). A new algorithm for surface deformation monitoring based on small baseline differential SAR interferograms. IEEE Transactions on Geoscience and Remote Sensing, **40**(11), 2375−2383.

33. Caskey, S.J. & A.R. Ramelli (2004). Tectonic displacement and far-field isostatic flexure of pluvial lake shorelines, Dixie Valley, Nevada. Journal of Geodynamics, **38**, 131–145.

34. Placzek, C., J. Quade & P.J. Patchett (2006). Geochronology and stratigraphy of late Pleistocene lake cycles on the southern Bolivian Altiplano: Implications for causes of tropical climate change,

Geological Society of America Bulletin, **11**8(5-6), 515-532.

35. Gosling, W. D., M.B. Bush, J.A. Hanselman & A. Chepstow-Lusty (2008). Glacial-Interglacial changes in moisture balance and the impacton vegetation in the southern hemisphere tropical Andes (Bolivia/Peru), Palaeogeography, Palaeoclimatology, Palaeoecology, **259**(1), 35-50.

36. Kraemer B, D. Adelmann, M. Alten, W. Schnurr, K. Erpenstein E. Kiefer, P. van den Bogaard & K. Görler (1999). Incorporation of the Paleogene foreland into Neogene Puna plateau: the Salar de Antofolla, NW Argentina. Journal of South Amrica Earth Sciences, **12**, 157–82.

37. Adelmann, D. (2001). Känozoische Becken-entwicklung in der südlichen Puna am Beispiel des Salar de Antofolla (NW-Argentinien). PhD thesis, Freie Universität Berlin.

38. Coutand, I., P.R. Cobbold, M. de Urreiztieta, P. Gautier, A. Chauvin, D. Gapais, E.A. Rossello & O. López-Gamundi (2001). Style and history of Andean deformation, Puna plateau, northwestern Argentina. Tectonics, **20**, 210-234.

39. Ruch, J., J.K. Warren, F. Risacher, T.R. Walter & R. Lanari (2012). Salt lake deformation detected from space. Earth and Planetary Science Letters **331-332**, 120-127.